

Effects of the Si-nanocluster size on the sensitizing role towards Er ions

F. Gourbilleau^a, R. Rizk, C. Dufour, and R. Madelon

SIFCOM, CNRS UMR 6176, ENSICAEN, 6 Boulevard du Maréchal-Juin, 14050 Caen Cedex, France

Received 12 December 2005 / Received in final form 20 April 2006

Published online 13 June 2006 – © EDP Sciences, Società Italiana di Fisica, Springer-Verlag 2006

Abstract. The effects of Si nanocluster (Si-nc) size on the energy transfer rate to Er ions were investigated through studies made on appropriate configurations of multilayers (MLs) consisting in about 20 periods of Er-doped Si-rich SiO₂/SiO₂. These MLs were deposited by reactive magnetron sputtering at 650 °C and subsequently annealed at 900 °C. For Si-rich layer thickness or Si-nc larger than about 4 nm, the sensitizing effect of Si-nc towards rare earth ions is highly lowered because of the weak confinement of carriers and the loss of resonant excitation of Er through the upper levels (second, third, ...). The latter is liable to prevent the energy back transfer process, while the weak confinement reduces strongly the probability of no phonon radiative recombination necessary for the energy transfer from Si-nc to Er ions.

PACS. 78.55.-m Photoluminescence, properties and materials – 78.67.Pt Multilayers; superlattices – 81.15.Cd Deposition by sputtering

The increasing need for combining both optical and electronic functionalities on the same Si-based chip, aims at reaching a true monolithic integration that allows, in turn, to solve several current issues relating to interconnect bottleneck, power dissipation, etc. [1]. One of the research directions explored during many years was the doping of silicon with Er, which is an interesting optical dopant emitting at the standard wavelength of 1.54 μm [2–4]. Such systems suffer, however, from two major deexcitation processes: (i) the phonon-assisted energy back-transfer originating from the near resonance between the Er-induced level in the band gap and the internal Er levels [3–5]; and (ii) the Auger-type interaction involving free carriers and excited Er ions [2]. The former induces a large temperature quenching in the photoluminescence (PL) intensity, while the latter increases with the density of excited carriers and gives rise also to energy backflow mechanism. To remove or reduce these detrimental effects, a promising approach is currently explored through the widening of the band gap by using silica as a host material co-doped with Er ions and Si nanoclusters (Si-nc) which turn out to be very efficient sensitizers of Er ions located within the most favourable chemical environment [6–8]. Among the various parameters governing the coupling between Si-nc and Er ion, such as the dynamics of the energy transfer (ET) from Si-nc to Er [9] and the characteristic interaction distance [10], the effects of Si-nc size, closely controlled by an appropriate approach, on the efficiency of the ET to Er ions deserve to be addressed. In this

respect, some studies [11–13] reported an increasing emission of Er when the Si-nc size is decreased (mostly below 5 nm), down to a value corresponding to tiny agglomerates of less than 50 Si atoms which are still efficient sensitizers [14]. However, a systematic and careful analysis is still lacking, especially the determination of the maximum size enabling the indirect excitation of Er, to optimize the material for high performance devices and to shed more lights on the physical mechanisms governing the ET rate. In this letter, we report on the PL properties of Er-doped multilayers (MLs) obtained by alternative deposition of Si-rich silicon oxide (SRSO) and silicon oxide (SO), typically of 20 periods. For the Er-doped SRSO/SO configuration, the variation of the SRSO thickness (t_{SR}) allows the control the Si-nc size, d_{Si} , growing within this sublayer and, therefore, enables a detailed investigation of d_{Si} effects on the ET efficiency.

The Er-doped MLs were deposited on Si substrates by sputtering the silica target alternatively under a plasma of 50% H₂ + 50% Ar to obtain the SRSO layer, owing to the ability of hydrogen to reduce oxygen, and under a plasma of pure Ar to obtain the SO layer. To incorporate the Er ions in SRSO (resp. SO) layers, the silica target sputtered with H₂ + Ar plasma (resp. Ar plasma) is topped by a specific number of Er₂O₃ chips. The MLs grown at 650 °C with a power density of 0.75 W cm⁻² were subsequently annealed at 900 °C for 1 h under a flux of N₂ mixed to 5% of H₂. According to secondary ion mass spectroscopy and Rutherford backscattering measurements, the Er concentration was around 4–6 × 10¹⁹ cm⁻³ and the Si excess close

^a e-mail: fabrice.gourbilleau@ensicaen.fr

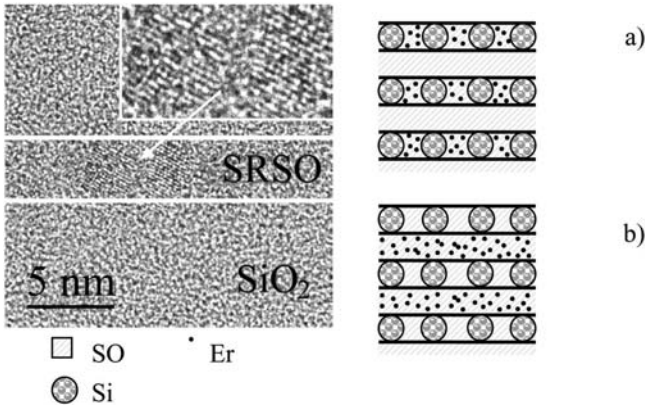


Fig. 1. Typical HRTEM image of the multilayers (MLs) for a 5-nm-thick Si-rich silicon oxide (SRSO) layer sandwiched between two silicon oxide (SO) layers and containing an array of Si nanocrystals. A magnified image of a nanocrystal is shown in the inset. Schematic drawings of the MLs showing Er in SRSO (a) and Er in SO (b).

to 11 at.%. The high resolution transmission electron microscopy (HRTEM) observations were made in a Topcon 002B on samples prepared in the cross-section configuration. The Er PL spectra were recorded at room temperature using a Ge detector cooled with liquid nitrogen, a grating monochromator and the usual lock-in technique. The out of resonance 476.5 nm line of an Ar laser, chopped at a frequency of 15 Hz was used to ensure only an indirect excitation of Er through the Si-nc. The excitation power was kept low (3 mW cm^{-2}) to remain in the linear regime of PL intensity vs power. Time-resolved Er PL was measured using a digitizing oscilloscope with an overall time response of about 0.5 ms.

Figure 1 reports a typical HRTEM image of a ML with $t_{\text{SR}} = 5.0 \text{ nm}$ showing evidence of Si nanocrystals formed within the SRSO layers and the schematic drawings of the structure with the two possible locations of Er ions. Although the crystallization of Si-nc is unnecessary for the sensitizing action [14,15], crystallized Si-nc are however observed for MLs with $t_{\text{SR}} \geq 3 \text{ nm}$. For thinner SRSO layers ($t_{\text{SR}} \leq 2 \text{ nm}$) no crystallization of Si-nc is observed (not shown), because it requires an annealing temperature much higher than $900 \text{ }^\circ\text{C}$ [16]. Anyway, all Si-nc, amorphous or crystallized formed within the SRSO layers of various t_{SR} values, are efficient sensitizers of Er ions located either in SRSO or SO layers. One expects, however, that Er ions are much closer to Si-nc in the former case and then benefit from a much more efficient sensitizing effect. To check this matter, we have recorded the PL spectra on both configurations, Er-doped SRSO/SO ML and SRSO/Er-doped SO ML, for the same thickness (3.8 nm) of SRSO and SO layers. The comparison of the PL spectra in the inset of Figure 2 shows ~ 40 times increase of the PL for Er located in SRSO layers instead of SO layers, hence confirming the closeness of Si-nc and Er in the former configuration. Consequently, the d_{Si} effects will be examined hereafter on Er-doped SRSO/SO superlattices through the variation of t_{SR} .

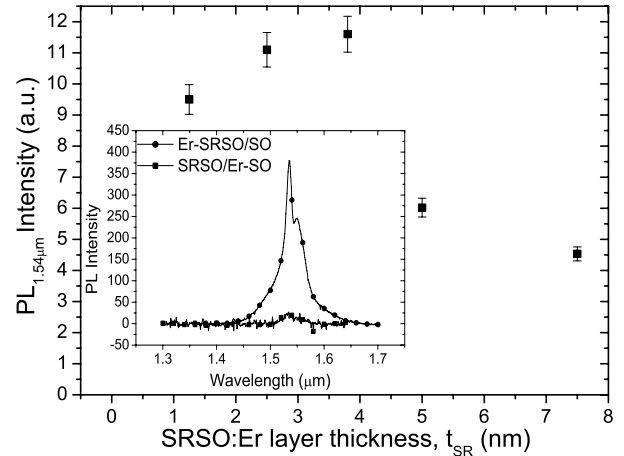


Fig. 2. Variation of the 1.54- μm PL intensity of the Er-doped SRSO/SO multilayers (MLs) in function of the SRSO layer thickness, t_{SR} . The lines have been added as guide to the eye. The inset compares the PL spectra recorded on Er-doped SRSO/SO and SRSO/Er-doped SO MLs with the indicated values of the various thicknesses.

Figure 2 shows the evolution of the PL intensity at 1.54 μm in function of t_{SR} . After an increase of about 20% for t_{SR} increasing from 1.2 to 3.8 nm, the emission reduces abruptly by half when t_{SR} exceeds 4 nm, before decreasing smoothly for $t_{\text{SR}} > 5 \text{ nm}$. The first moderate increase with t_{SR} or d_{Si} ($< 4 \text{ nm}$) can originate from the concomitant increase of the absorption cross section of Si-nc sensitizers [17], and is also compatible with the maximum quantum yield observed in similar MLs for $d_{\text{Si}} = 3 - 4 \text{ nm}$ [13]. However, the strong decrease occurring for $t_{\text{SR}} \geq 4 \text{ nm}$ is a clear indication of a size effect which can be due to either or both reasons:

- (i) the growth of some Si-nc as large as $t_{\text{SR}} \geq 4 \text{ nm}$, as expected, gives rise to d_{Si} comparable or larger than the exciton ‘Bohr radius’ estimated to 5 nm for silicon. This leads to a weak carrier confinement that lowers the excited level of Si-nc which becomes no more resonant with the upper excited levels of Er. Note that there are still numerous Si-nc with a size smaller than t_{SR} , since the PL decreases to the third without vanishing when t_{SR} increases from 3.8 to 7.5 nm;
- (ii) the second origin lies in the possible presence of Er within the large Si-nc, which might lead to the already mentioned deexcitation processes encountered in bulk c-Si. These detrimental processes are, in fact, favoured by the increase of d_{Si} , the subsequent shrinkage of the bandgap and the higher content of carriers density.

To elucidate these aspects and give further insights concerning the origin of the observed PL decrease for $t_{\text{SR}} \geq 4 \text{ nm}$ (Fig. 2), the temperature dependences of PL intensity I_{PL} and lifetime τ at 1.54 μm were measured from 10 K to 300 K for different t_{SR} values. The evolutions of both I_{PL} and τ in function of the temperature are displayed in Figures 3a and 3b, respectively. They are also compared to their counterparts from a single Er-doped

Table 1. Ratios of the 1.54- μm PL intensity and emission lifetime at 10 K and 300 K, $I(10\text{ K})/I(300\text{ K})$ and $\tau(10\text{ K})/\tau(300\text{ K})$, respectively, for different thicknesses of the Er-doped SRSO layer of the multilayers. The corresponding ratios obtained on Er-doped bulk Si crystal are also reported for comparison, according to references [3] and [4], together with those measured on 530-nm-thick single SRSO layer grown similarly by reactive magnetron sputtering.

Sample	$I(10\text{ K})/I(300\text{ K})$	$\tau(10\text{ K})/\tau(300\text{ K})$
Er-doped Bulk (monocrystalline Si)	1000 (Refs. [3,4])	140 (Ref. [3])
$t_{\text{SR}} = 2.5\text{ nm}$	3.3	1.1
$t_{\text{SR}} = 3.8\text{ nm}$	2.5	1.3
$t_{\text{SR}} = 5\text{ nm}$	3.7	1.2
530-nm-thick single Er ³⁺ doped SRSO layer	3	1.1

SRSO layer as thick as 530 nm, considered as a reference. It can be noticed that the thermal quenching, if any, is far from being comparable to that reported for Er-doped bulk-Si crystal, for both I_{PL} [3,4] and τ [3], according to the ratios $I_{\text{PL}}(10\text{ K})/I_{\text{PL}}(300\text{ K})$ and $\tau(10\text{ K})/\tau(300\text{ K})$ reported in Table 1. The intensity ratios (around 2–4) are equivalent to that reported for similar MLs [13] and are also comparable to that of the reference thick single layer. For all our MLs and also for the reference sample, we deal, therefore, with a Si-nc-mediated excitation of Er, since the intensity ratios are all much smaller than that (10^3) reported for the Er-doped bulk c-Si [4], indicating the absence of significant deexcitation processes such those observed for bulk c-Si and which would be induced by an eventual presence of Er within large Si-nc. Anyway, such a presence would imply an Er concentration close to the solubility limit of Er in Si ($\approx 10^{19}\text{ cm}^{-3}$). The strong sensitizing action of Si-nc seems also to reduce the nonradiative decay channels for all MLs and reference film, because the relating lifetimes do not significantly change between 10 and 300 K, as observed earlier for similar Er coupled Si-nc systems [8].

The PL decrease for $t_{\text{SR}} \geq 4\text{ nm}$ (Fig. 2) reflecting some lowering of ET rate would be due to the shrinkage of the bandgap and the subsequent mismatch between the exciton PL band and the upper excited levels of Er. This shrinkage is also accompanied by some release of the carriers quantum confinement which has been closely correlated to the probability of no phonon radiative recombination P_{NP} [18]. For low d_{Si} (or t_{SR}), P_{NP} is expected to dominate at the expense of the phonon-assisted counterpart P_{PA} , particularly the TO one [12,19]. A high $P_{\text{NP}}/P_{\text{PA}}$ ratio reflects, therefore, a strong localization of carriers and a partial breaking of the k -conservation, which are further strengthened for Si-nc having an abrupt Si/SiO₂ interface [20]. This implies that amorphous Si-nc formed for $t_{\text{SR}} \leq 2.0\text{ nm}$ and crystalline Si-nc grown for $2\text{ nm} < t_{\text{SR}} \leq 3.8\text{ nm}$ have comparable $P_{\text{NP}}/P_{\text{PA}}$ ratios [18], hence supporting the earlier suggestion of ascribing the improvement of I_{PL} in this range to the increase of the absorption cross section of Si-nc [17]. Since P_{NP}

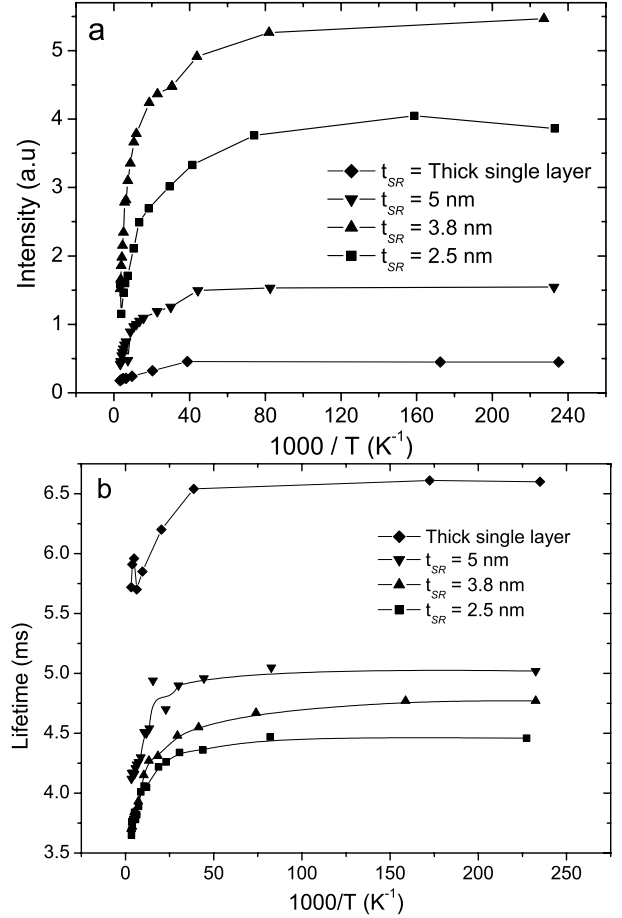


Fig. 3. The intensity of the 1.54- μm peak (a) and the emission lifetime (b) as a function of temperature, for some typical thicknesses of the Er-doped SRSO layer of the multilayers. The corresponding plots for the 530-nm-thick single SRSO layer are also reported.

is assumed as governing the ET rate [12], the number of excited Er ions, N_{Er}^* , or correspondingly I_{PL} , can be considered as \propto to P_{NP} and, therefore, as $d_{\text{Si}}^{-\alpha}$ ($\alpha > 1$ deserving determination), as attested by the ranking of I_{PL} for the different t_{SR} values in Figure 3a. The abrupt drop observed for $t_{\text{SR}} > 4\text{ nm}$ is quite coherent with the low value of $P_{\text{NP}}/P_{\text{PA}}$ ratio, ~ 0.02 , reported for Si-nc size exceeding 5 nm for which a weak confinement prevails [18]. In this case, the widening of the bandgap leads to a mismatch between the excited level of nc-Si and the upper excited levels of Er ($I_{11/2}$, $I_{9/2}$), resulting in a substantial weakness of the exchange interaction suspected to govern the ET process from nc-Si to Er [10]. The PL intensity remains, however, significantly higher than that of the reference thick single SRSO layer containing much larger size distribution. The emission lifetime τ appears almost unaffected by the temperature change with a ratio $\tau(10\text{ K})/\tau(300\text{ K}) \sim 1.1\text{--}1.3$. This contrasts strongly with the large variation (more than two orders of magnitude) observed for Er-doped bulk c-Si [3]. Contrary to the case of I_{PL} , the reference single layer presents high values of τ , between 5.7 and 6.5 ms, away from the lower values of τ ,

for the MLs. The origin of this behaviour is lying, most likely, in the density of nonradiative defects located at interfaces such as those between Si-nc and the surrounding silica within the SRSO layers and those prevailing between successive SRSO/SO layers. These latter seems to play a key role in the reduction of the lifetime, since their absence in the reference single layer can explain the corresponding highest value of the lifetime. The slight trend of τ , lowering for decreasing values of t_{SR} might originate from the concomitant enhancement of the surface/volume ratio for Si-nc.

The two parameters I_{PL} and τ are highly important for device performance. Indeed, the optical gain g is \propto to the product $\sigma_{\text{em}} \times N_{\text{Er}}^*$ with $N_{\text{Er}}^* \propto (I_{\text{PL}} \times \tau_{\text{rad}}) / \tau$ (τ_{rad} : radiative lifetime) and σ_{em} the emission cross section being $\propto 1/\tau_{\text{ra}}$, resulting in $g \propto I_{\text{PL}}/\tau$. By comparing the g value for the ML with $t_{\text{SR}} = 2.5$ nm to the corresponding one for the reference single layer, we notice a potential improvement of the optical gain of nearly an order of magnitude for the ML. Such a benefit is clearly due to the enhanced intensity for the MLs which control somehow the size of the growing Si-nc and then optimize their coupling with Er, hence underlying the relevance of using ML structure for the fabrication of active devices.

In summary, this work reports a study aiming at examining the impact of Si-nc size on the efficiency of their coupling with Er ions. We found that for a size exceeding 4 nm, the combined and interrelated effects of both bandgap widening and lowering of the quasi direct radiative recombination of excitons are responsible of the abrupt drop in the emission intensity of Er ions. For $t_{\text{SR}} > 4$ nm, the excited level of nc-Si is, indeed, no more matching with any of the upper excited level of Er ($I_{11/2}$, $I_{9/2}$), leading to some inefficiency of the exchange interaction. The small PL temperature quenching indicates, on the one hand, the presence of Er outside Si-nc and, on the other hand, the excitation (if any) of the upper levels of Er. This latter becomes naturally possible for a Si-nc band gap larger than a threshold value, implying a small energy back transfer process. These results allow the optimization of the concentrations of both emitting centers (Er ions) and sensitizers (Si-nc) for efficient emission and possible realization of active device.

This work was supported by the EU SINERGIA project (IST 2000-29650).

References

1. *E-MRS Proceedings Symposium on Si-based Photonics: Towards True Monolithic Integration* [Optical Materials (2005)]
2. J. Michel, J.L. Benton, R.F. Ferrante, D.C. Jacobsen, D.G. Eaglesham, E.A. Fitzgerald, Y.-H. Xie, J.M. Poate, L.C. Kimerling, *J. Appl. Phys.* **70**, 2672 (1991)
3. P.G. Kik, M.J.A. de Dood, K. Kikoin, A. Polman, *Appl. Phys. Lett.* **70**, 1721 (1997)
4. F. Priolo, G. Franzò, S. Coffa, A. Carnera, *Phys. Rev. B* **57**, 4443 (1998)
5. A. Tagushi, K. Takahei, *J. Appl. Phys.* **83**, 2800 (1998)
6. A.J. Kenyon, P.F. Trwoga, M. Federighi, C.W. Pitt, *J. Phys. Condens. Matter.* **6**, L319 (1994)
7. M. Fujii, M. Yoshida, S. Hayashi, K. Yamamoto, *J. Appl. Phys.* **84**, 4525 (1998)
8. G. Franzò, V. Vinciguerra, F. Priolo, *Appl. Phys. A: Mater. Sci. Process.* **69**, 3 (1999)
9. M. Fujii, K. Imakita, K. Watanabe, S. Hayashi, *J. Appl. Phys.* **95**, 272 (2004)
10. J.H. Jhe, J.H. Shin, K.J. Kim, D.W. Moon, *Appl. Phys. Lett.* **82**, 4489 (2003)
11. J. Heitmann, M. Schmidt, M. Zacharias, V. Yu Timoshenko, M.G. Lisachenko, P.K. Kashkarov, *Mater. Sci. Engin. B* **105**, 214 (2003)
12. K. Watanabe, M. Fujii, S. Hayashi, *J. Appl. Phys.* **90**, 4761 (2001)
13. V. Yu. Timoshenko, M.G. Lisachenko, B.V. Kamenev, O.A. Shalygina, P.K. Kashkarov, J. Heitman, M. Schmidt, M. Zacharias, *Appl. Phys. Lett.* **84**, 2512 (2004)
14. G. Franzò, S. Boninelli, D. Pacifici, F. Priolo, F. Iacona, C. Bongiorno, *App. Phys. Lett.* **82**, 3871 (2003)
15. F. Gourbilleau, C. Dufour, M. Levalois, J. Vicens, R. Rizk, C. Sada, F. Enrichi, G. Battaglin, *J. Appl. Phys.* **94**, 3869 (2003); F. Gourbilleau, M. Levalois, C. Dufour, J. Vicens, R. Rizk, *J. Appl. Phys.* **95**, 3717 (2004)
16. L.X. Yi, J. Heitmann, R. Scholtz, M. Zacharias, *Appl. Phys. Lett.* **81**, 4248 (2002)
17. D. Kovalev, J. Diener, H. Heckler, G. Polisski, N. Künzner, F. Koch, *Phys. Rev. B* **61**, 4485 (2000)
18. D. Kovalev, H. Heckler, M. Ben-Chorin, G. Polisski, M. Schwartzkopff, F. Koch, *Phys. Rev. Lett.* **81**, 2803 (1998)
19. V. Yu. Timoshenko, M.G. Lisachenko, O.A. Shalygina, B.V. Kamenev, D.M. Zhigunov, S.A. Teterukov, P.K. Kashkarov, J. Heitman, M. Schmidt, M. Zacharias, *J. Appl. Phys.* **96**, 2254 (2004)
20. V.A. Kharchenko, M. Rosen, *J. Lumin.* **70**, 158 (1996)